Enabling Cooperative Relaying VANET Clouds Over LTE-A Networks

Mohamed F. Feteiha, *Member, IEEE*, and Hossam S. Hassanein, *Senior Member, IEEE*

Abstract—This paper addresses the area of heterogeneous wireless relaying vehicular clouds. We devise an advanced vehicular relaying technique for enhanced connectivity in densely populated urban areas. We investigate the performance of a transmission scheme over a Long-Term Evolution-Advanced (LTE-A) network where vehicles act as relaying cooperating terminals for a downlink session between a base station and an end-user. The abundance of moving vehicles, operating in an ad hoc fashion, can eliminate the need for establishing a dedicated relaying infrastructure. However, the associated wireless links in vehicular clouds are characterized by a doubly selective fading channel; this causes performance degradation in terms of increased error probability. Hence, we propose a precoded cooperative transmission technique to extract the underlying rich multipath–Doppler-spatial diversity, which is a relay selection scheme to take advantage of the potentially large number of available relaying vehicles. We further contribute by the derivation of a closed-form error rate expression, diversity gain, and outage expressions and introduce our derived performance unconditional expressions as a benchmark to assess our analysis and future research studies of such an approach. Our analytical and simulation results indicate that significant diversity gains and reduced error rates are achievable. In addition, there is a noticeable reduction in the required transmitting power compared with traditional transmission schemes, as well as an increase in distance coverage.

Index Terms—Best relay selection, cooperative relaying, fourth generation (4G), Long-Term Evolution-Advanced (LTE-A), vehicular ad hoc network (VANET), vehicular communications.

I. INTRODUCTION

IN cellular networks, inherent limitations on cell capacity and cell coverage exist. Due to the capacity limitation, in dense urban areas, such as downtown areas and major events, users tend to experience degraded performance. In the search for ways to enhance network performance, researchers have turned their attention to vehicles on the road. The abundant onboard vehicle resources [1] that are underutilized by traditional vehicular applications offer an opportunity for improved computing and connectivity in vehicular ad hoc networks (VANETs) [2]. Indeed, with its diverse resources, including sensing, processing, storage, and communication modules, a vehicle can be a potentially excellent candidate as a "mobile relay" to support what we call relaying vehicular cloud networking (RVC-Net). We propose the creation of a "cooperative RVC-Net" using vehicles equipped with short- and medium-range wireless communication technologies and low elevation antennas. The main reason for using vehicles as relays is to reduce power consumption at the end-user mobile terminal. By reducing the distance between the transmitter and the receiver, the required transmission power is also reduced. Unlike base stations (BSs), relay stations (RSs) are less complex and do not require wired backbone access. In addition, RSs provide higher throughput, increase coverage, lower operational and capital expenditure, allow for faster communication links to roll out, and offer a more flexible configuration. Cooperative RVC-Net can be an integral part of the next-generation cellular network, namely, Long-Term Evolution-Advanced (LTE-A); LTE-A is the *de facto* fourth-generation (4G) wireless system and is expected to dominate the next generation of wireless networks and to support a wide variety of applications that require higher data rates with more reliable transmission. To meet such demands, wireless communication system designers need to optimize network performance in terms of better link reliability, fewer dropped connections, and longer battery life [3]. LTE-A was ratified by the International Telecommunication Union as an International Mobile Telecommunications-Advanced (IMT-Advanced) 4G technology in November 2010 and has adopted relaying for cost-effective throughput enhancement and coverage extension [4], [5].

The utilization of the proposed cooperative RVC-Net architecture is aimed at increasing network performance without the expense of expanding network infrastructure. We remark that user cooperation has been recently applied to vehicular communications to extend coverage, enable ad hoc connectivity, and enhance link reliability through distributed spatial diversity [6]–[12]. To motivate vehicles to act as cooperative relays, incentive mechanisms for multiuser cooperative relaying have been proposed in the literature [13].

The main challenge facing the deployment of vehicular relaying networks manifests itself in the systems advantage, which is the lack of infrastructure. For such types of networks, the physical-layer designs have to cope with tremendous challenges, including an extendable relaying network area over the entire road with many participants and an extremely dynamic environment with a topology that is always changing. Furthermore, due to the high speed of moving vehicles, the

connectivity of the vehicular relaying could be compromised, changing frequently, which causes a higher probability of disconnection. As well in LTE-A wireless broadband vehicular relaying, intersymbol interference (ISI) introduces frequency selectivity, whereas Doppler spreads result in time selectivity. To realize the full potential of cooperative diversity using vehicular relaying networks, it is important to conduct an in-depth investigation of performance limits and develop enabling techniques to support such broadband transmission. In this paper, we investigate the performance gains of a transmission scheme in LTE-A networks where vehicles act as relaying cooperating terminals for an eNodeB-to-User Equipment (UE) downlink session. The associated wireless links are characterized by a doubly selective fading channel, which results in performance degradation, in terms of increased error probability. Hence, we propose a precoded cooperative transmission technique to extract the underlying rich multipath–Doppler–spatial diversity. Furthermore, we implement a best relay selection scheme to take advantage of the potentially large number of available relaying vehicles. We further contribute by

1) devising an effective precoding transmission scheme and a relay selection technique that significantly increase diversity gains and reduce error rates;
2) the derivation of closed-form formulas for error rate and outage probability as a benchmark to assess our analysis and future research studies of such an approach;
3) demonstrating the performance gains of the proposed approach, analytically and through simulation, compared with the traditional approaches.

The remainder of this paper is organized as follows. In Section II, we describe the proposed two-phase dual-hop cooperative system using a best relay selection from M available vehicles willing to be involved in the transmission session. In Section III, we derive a closed-form expression for the pairwise error probability (PEP) and demonstrate the achievable diversity gains. In Section IV, we derive the outage probability closed-form expression. In Section V, we present numerical results to confirm the analytical derivations and provide insight into the system performance. Section VI concludes this paper.

Notations: $(.)^T$, $(.)^*$, and $(.)^H$ denote transpose, conjugate, and Hermitian operations, respectively. $\mathbb{E}[.]$, $\|.\|$, and $\otimes$ denote expectation, absolute value, and Kronecker product, respectively. Bold letters denote the matrices and vectors. $[\mathbf{H}]_{k,m}$ represents the (k, m)th entry of $\mathbf{H}$. $\mathbf{I}_N$ indicates an $N \times N$-size identity matrix. $\mathbf{1}$ and $\mathbf{0}$ represent, respectively, all-ones and all-zeros matrix with proper dimensions. $\lceil . \rceil$ and $\lfloor . \rfloor$ denote integer ceil and integer floor operations, respectively. $*$ is the convolution operator. x, i, j, k are dummy variables. $F(.)$ and $f(.)$ are the cumulative distribution function (cdf) and the probability density function (pdf) for a given random variable, respectively. The distances, geometrical gains, and path-loss coefficient are denoted by $d_{(.)}$, $G_{(.)}$, and α, respectively. $L_{(.)}$ denotes the number of multipath, and $\mathcal{Q}_{(.)}$ denotes the number of Doppler shifts. The number of available relaying vehicles willing to contribute in transmission is given by M. We have P and Z as the precoder design parameters.

II. SYSTEM MODEL

There are two main approaches to handle cooperative communications. The first approach involves adaptive transmission in which one or more transmission parameters (coding, modulation, power, etc.) are varied according to the channel conditions. This builds on a closed-loop implementation in which feedback from the receiver to the transmitter is required. The second approach is the use of either outer coding or precoding. These are open-loop implementations that do not require feedback. Such techniques are particularly useful over time-varying channels where reliable feedback is difficult to obtain. In our paper, considering the time-selective nature of the vehicular system under consideration, we used the linear constellation precoding approach. Such an approach is particularly useful over high-speed mobility communications, where reliable feedback is difficult to obtain. Taking this into consideration, we will build our communication scheme over orthogonal transmission protocol, cooperative relaying, as well as outer and linear signal precoding.

The utilization of multihop relaying techniques is aimed at increasing network performance without the high costs of expanding a networks' infrastructure. The main principle in relaying results in reduced levels of power consumption for the mobile terminals. This is the outcome of reducing the transmitter-to-receiver distance and, hence, the required transmission power. Unlike BSs, RSs are less complex and do not require wires for the backbone access. In addition, they provide higher throughput, increase coverage, lower operational and capital expenditure, allow for faster roll out, and offer a more flexible configuration. An alternate approach for relaying is by making use of vehicles equipped with low elevation antennas and short- and medium-range wireless communication technologies.

Adopting such transmission model will directly utilize five inherent advantages of vehicular networking.

1) There is abundant energy and computing power (including both storage and processing).
2) There are predictable movement patterns of vehicles as they are in most cases limited to roads.
3) Road map information is often available from positioning systems and map-based technologies such as GPS.
4) The trajectory of a vehicle can be predicted given the average speed, current speed, and road map.
5) The frequent availability of traveling vehicles, operating in an ad hoc fashion, eliminates the need for establishing a dedicated relaying infrastructure.

With its diverse resources, including sensing, processing, storage, and communication modules, a vehicle can offer a distributed system that can manage signal processing tasks in a faster and a more efficient way than centralized computing. Although the expectations for this emerging technology are set very high, many practical aspects still remain unsolved for a vast deployment of vehicular networks. A vehicle can offer a distributed system that can manage cooperative relaying tasks in a more efficient way than a roadside dedicated relay by deploying a precoded transmission that can extract the rich underlying multipath–Doppler diversity. The Doppler diversity
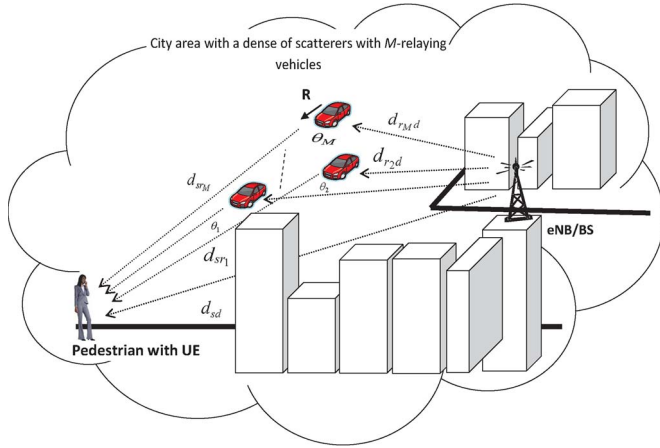
Fig. 1. Cooperative vehicular communication over LTE-A, using M-relay deployment.

is the outcome of the Doppler shifts resulting from the high-speed vehicle mobility.

We consider a cooperative communication scenario, as shown in Fig. 1, where an eNodeB antenna (source) directly communicates with UE (destination) and indirectly through a relaying vehicle (R) that serves as a best selected relaying terminal. All terminals are assumed to be equipped with single transmit-and-receive antennas and operate in half-duplex mode. We assume the orthogonal cooperation protocol of with decode-and-forward (DF) relaying [14]. In the broadcasting phase, the source (antenna) transmits its precoded signal to the relaying vehicle (R) and to the destination (UE). In the relaying phase, the relay is engaged in forwarding the received signal only if it was decoded correctly; otherwise, the relay is silent. The relay decodes and then forwards a newly decoded copy of the precoded signal to the destination. The destination makes its decision based on the two received signals over the broadcasting and relaying phases.

When the transmitter vehicle and/or the receiver vehicle are in motion, the Doppler phase shift, i.e., the amount of change in the frequency due to the vehicles' relative mobility, must be taken into account. Ignoring the additive noise, the bandpass received signal can be written as [15], [16]

$$\mathcal{Y}(t) = \mathrm{Re}\left\{\sum_{n=1}^{\mathcal{N}(t)} \alpha_n(t) s_l\left(t - \tau_n(t)\right) e^{j(2\pi f_c + \omega_{D_n}(t))(t - \tau_n(t))}\right\} \tag{1}$$

or, equivalently, the impulse response as

$$h(\tau, t) = \sum_{n=1}^{\mathcal{N}(t)} \alpha_n(t) e^{j((\omega_{D_n}(t))(t - \tau_n(t)) + 2\pi f_c \tau_n(t))} \delta\left(\tau - \tau_n(t)\right). \tag{2}$$

In the foregoing equations, $\mathcal{N}(t)$ is the number of resolvable multipath components, $\alpha_n(t)$ is the attenuation factor of the nth path, $s_l(t)$ is the equivalent low-pass signal, $\tau_n(t)$ is the delay associated with the nth path, f_c is the carrier frequency, and

$\omega_{D_n}(t)$ is the Doppler phase shift associated with the nth path due to the mobility and is given by

$$\omega_D(t) = 2\pi f_D(t) = \frac{2\pi}{\lambda} v(t) \cdot \cos(\vartheta) \tag{3}$$

where ϑ is the signal's angle to the vehicle, $v(t)$ is the vehicle's velocity, λ is the wavelength of the carrier, and $f_D(t)$ is the Doppler shift. The difference between the Doppler shifts in various signal components (contributing to a single fading channel tap) forms the Doppler spread of the channel and is given by $f_d = 1/T_d$, where T_d is the coherence time of the channel.

Jakes' model assumes an isotropic rich scattering around the mobile receiver antenna and builds upon a *single-ring model*. In this model, the angles of arrival ϑ of the waves arriving at the receiving antenna are uniformly distributed in the interval of $[-\pi, \pi]$. This single-ring model is generally used for cellular systems that typically involve a stationary BS antenna above the rooftop level unobstructed by the local scatterers.

In highly scattered areas, there are a large number of paths along with the absence of a dominating line-of-sight path. The central limit theorem suggests that the complex fading coefficient can be modeled as zero-mean complex Gaussian. Therefore, the envelope of the channel follows a Rayleigh distribution, whereas the phase is uniformly distributed [17]. In vehicle-to-vehicle communication, the antenna is close to the ground level (1.5–2.5m) and is dynamic with higher speed and variation, which requires considering the local scattering around the vehicular antenna. In [18], Akki and Haber considered a scattering model surrounding the mobile terminals with omnidirectional antennas, assuming two communicating terminals moving with velocities v_1 and v_2. For this mobility scenario, each path will be subject to separate Doppler shifts, yielding to the impulse response [18], i.e.,

$$h(\tau, t) = \sum_{n=1}^{\mathcal{N}(t)} \alpha_n(t) e^{j((\omega_{D1_n}(t) + \omega_{D2_n}(t))(t - \tau_n(t)) + 2\pi f_c \tau_n(t))}$$
$$\times \delta\left(\tau - \tau_n(t)\right) \tag{4}$$

where $\omega_{D1_n}(t)$ and $\omega_{D2_n}(t)$ are the Doppler phase shifts introduced by the two mobile vehicles. Here, the delay term can be expressed as

$$\tau_n(t) = \tau_i + \delta_{\tau_n}(t) \tag{5}$$

where τ_i is the mean value of multipath time delay, and $\delta_{\tau_n}(t)$ is the time delay difference for the nth path measured from that mean value. We can then express (5) as

$$h(\tau, t) = \sum_{n=1}^{\mathcal{N}(t)} \alpha_n(t) e^{j((\omega_{D1_n}(t) + \omega_{D2_n}(t))(t - \tau_i) + 2\pi f_c \tau_i + \phi_n)}$$
$$\times \delta\left(\tau - \tau_i - \delta_{\tau_n}(t)\right). \tag{6}$$

In (6), $\phi_n = (2\pi f_c + \omega_{D1_n}(t) + \omega_{D2_n}(t))\delta_{\tau_n}(t)$ is uniformly distributed in $[0, 2\pi)$. The time correlation function is given by

$$C(\Delta t) = \sigma^2 J_0\left(\frac{2\pi}{\lambda} v_2 \Delta t\right) J_0\left(\frac{2\pi}{\lambda} v_1 \Delta t\right) \tag{7}$$

with t_1 and t_2 referring to the two different time instants, and we have $\Delta t = t_2 - t_1$. The zero-order Bessel function is J_0, λ is the wavelength of the carrier frequency, and σ^2 is the channel variance. The power spectrum of the complex envelope is given by

$$S(f) = \frac{\sigma^2}{\pi^2 f_{D1_m} \sqrt{\eta}} K \left[\frac{(1+\eta)}{2\sqrt{\eta}} \sqrt{1 - \left(\frac{f}{(1+\eta)f_{D1_m}} \right)^2} \right] \tag{8}$$

where $\eta = v_2/v_1$, f_{D1_m} is the maximum Doppler shift due to the motion of the transmitter, and $K[.]$ is the complete elliptic integral of the first kind. For $\eta = 0$ (i.e., $v_2 = 0$), the power spectrum and time correlation functions reduce back to Jakes' model.

Our aggregate channel model takes into account both small-scale fading and path loss. Path loss is proportional to d^α, where α is the path-loss coefficient and d is the propagation distance. The path loss associated with the distance d from the eNodeB to the UE is modeled as [19]

$$\Omega(d) = 10^{(128.1 - 36.7 \log_{10} d)/10}. \tag{9}$$

Let d_{sd} denote the distance from source S to destination D $(S \rightarrow D)$, with d_{sr_i} and $d_{r_i d}$, respectively, denoting, the distances $(S \rightarrow R_i)$ and $(R_i \rightarrow D)$, $i = 1, 2, \ldots, M$. θ_i is the angle between lines $S \rightarrow R_i$ and $R_i \rightarrow D$. The relative geometrical gains are defined as $G_{sr_i} = (d_{sd}/d_{sr_i})^\alpha$ and $G_{r_i d} = (d_{sd}/d_{r_i d})^\alpha$ and can be further defined using the law of cosines as $G_{sr_i}^{-2/\alpha} + G_{rd_i}^{-2/\alpha} - 2G_{sr_i}^{-2/\alpha} G_{r_i d}^{-2/\alpha} \cos \theta_i = 1$.

As for short-term fading, it should be noted that relaying vehicles R and destination UE have low elevation antennas and are located within a highly scattering urban area. This requires considering the local scattering around transmitters and receivers. The time correlation function is given by

$$C(\Delta t) = \sigma^2 J_0 \left(\frac{2\pi}{\lambda} v_e \Delta t \right) J_0 \left(\frac{2\pi}{\lambda} v_r \Delta t \right) \tag{10}$$

where v_r and v_e are the velocities of the two communicating terminals. We have a stationary eNodeB antenna (i.e., $v_e = 0$). Assuming a single Rayleigh distribution with a single Doppler shift, the power spectrum and time correlation mathematical functions reduce to having the autocorrelation function and the power spectrum of the complex envelope. These are, respectively, given by $C(\tau) = \sigma^2 J_0(2\pi v_r \tau/\lambda)$ and $S(f) = \sigma^2(\pi f_{D_m} \sqrt{1 - (f/f_{D_m})^2})^{-1}$, with v_r being the maximum velocity of relaying vehicles. In addition to time-selectivity results from the Doppler shifts, the channel is subject to frequency selectivity quantified through delay spread τ_d. The channel satisfies the condition $2f_d \tau_d < 1$ [20]. Note that in the vehicular channel, there are several instantaneous velocities due to the acceleration/decelerations. The earlier defined maximum Doppler shift f_{D_m} has been therefore calculated based on the maximum velocities experienced.

The block diagram of the proposed cooperative scheme is shown in Fig. 2. The input data blocks $s(i)$ (generated from an M-ary quadratic-amplitude modulation constellation) of length
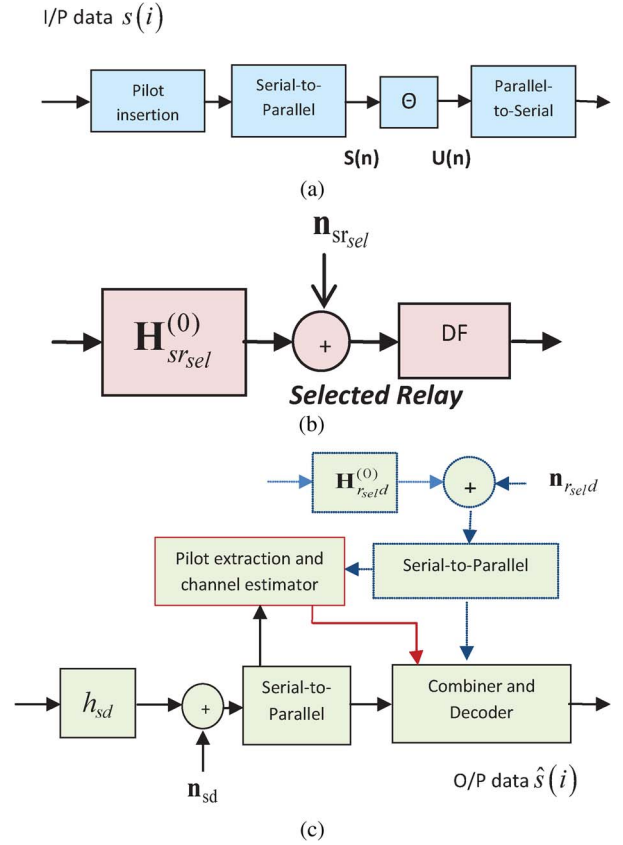

Fig. 2. Block diagram for (S), (R), and (D). (a) eNodeB (source). (b) Selected relaying vehicle. (c) UE (destination).

N_t are divided into shorter subblocks of length N_s ($N_s \le N_t$). Let each of these subblocks be denoted by $\mathbf{s}(n)$, which are the input to a linear precoder Θ of size $N_s \times N_t$. We have $N_s = PZ$ and $N_t = (P+Q)(Z+L)$. The number of the resolvable multipath components is given by $L = \lceil \tau_d/T_s \rceil$, and the number of Doppler shifts experienced over the data block is given by $Q = \lceil N_t T_s f_d \rceil$; we have T_s as the symbol duration. The time-sampled orthogonal frequency-division multiplexing signal is converted into the frequency domain by implementing a discrete Fourier transform (DFT). The DFT renders a discrete finite sequence of complex coefficients. We choose the number of coefficients equal to $Q + 1$, and the signal is given by

$$[\mathbf{s}(n)]_q = s(q)e^{-jw_q}, \qquad q = 0, 1, \ldots, Q \tag{11}$$

where $w_q = 2\pi(q - Q/2)/N_t$ is the finite Fourier bases that capture the time variation. From (11), the basis expansion model can be used to represent a discrete-time baseband equivalent channel for the vehicular doubly selective channel under consideration and is given by

$$h_B(\ell; l) = \sum_{q=0}^{Q} h_q(n; l)e^{j2w_q \ell}, \qquad l \in [0, L] \tag{12}$$

where $h_q(n; l)$ is zero-mean complex Gaussian. Here, ℓ denotes the serial index for the input data symbols. The block index is given by $n = \lfloor \ell/N_t \rfloor$. For the cooperative scheme under

consideration, define $\mathbf{H}_{sd,q}^{(0)}$, $\mathbf{H}_{sr,q}^{(0)}$, and $\mathbf{H}_{rd,q}^{(0)}$ as the lower triangular Toeplitz channel matrices with entries given by (12). Let L_{sd}, L_{sr}, and L_{rd} denote the channel multipath lengths for the S → D, S → R, and R → D links, respectively. Further, let $\mathcal{Q}_{sd}$, $\mathcal{Q}_{sr}$, and $\mathcal{Q}_{rd}$ denote the number of resolvable Doppler components for corresponding links.

In the broadcasting phase, the received signals at the relay can be expressed in a matrix form as

$$\mathbf{y}_{sr}(n) = \sqrt{G_{sr}E_s} \sum_{q=0}^{Q} \mathbf{D}(w_q)\mathbf{H}_{sr,q}^{(0)}(n)\mathbf{u}(n) + \mathbf{n}_{sr}(n) \quad (13)$$

where $\mathbf{u}(n) = \boldsymbol{\Theta}\mathbf{s}(n)$ is the transmitted data block, $Q = \max(\mathcal{Q}_{sd}, \mathcal{Q}_{sr}, \mathcal{Q}_{rd})$, and E_s is the modulated symbol energy. We have $\mathbf{D}(w_q) := \text{diag}[1, \ldots, \exp(jw_q(N_t - 1))]$, and $\mathbf{n}_{sr}(n)$ is the S → R additive white Gaussian noise (AWGN) vector with entries of zero mean and $N_0/2$ variance. Using the commutativity of products of Toeplitz matrices with vectors, we can replace $\mathbf{H}_{sr,q}^{(0)}(n)\mathbf{u}(n)$ with $\mathbf{U}(n)\mathbf{h}_{sr,q}(n)$ and rewrite (13) as

$$\mathbf{y}_{sr}(n) = \sqrt{G_{sr}E_s} \sum_{q=0}^{Q} \mathbf{D}(w_q)\mathbf{U}(n)\mathbf{h}_{sr,q}(n) + \mathbf{n}_{sr}(n). \quad (14)$$

Defining the augmented matrices

$$\mathbf{h}_{sr}(n) = \begin{bmatrix} \mathbf{h}_{sr,0}^{\mathrm{T}}(n) & \cdots & \mathbf{h}_{sr,Q}^{\mathrm{T}}(n) \end{bmatrix}^{\mathrm{T}}$$

$$\boldsymbol{\Phi}(n) = \begin{bmatrix} \mathbf{D}(w_0)\mathbf{U}(n) & \cdots & \mathbf{D}(w_Q)\mathbf{U}(n) \end{bmatrix}$$

we have

$$\mathbf{y}_{sr}(n) = \sqrt{G_{sr}E_s}\,\boldsymbol{\Phi}(n)\mathbf{h}_{sr}(n) + \mathbf{n}_{sr}(n). \quad (15)$$

Similarly, the received signal at the destination during the broadcasting phase is given by

$$\mathbf{y}_{sd}(n) = \sqrt{E_s}\,\boldsymbol{\Phi}(n)\mathbf{h}_{sd}(n) + \mathbf{n}_{sd}(n) \quad (16)$$

where $\mathbf{n}_{sd}(n)$ is the associated S → D AWGN vector with entries of zero mean and $N_0/2$ variance. During the relaying phase, the relay-received signals are fed to the maximum-likelihood (ML) detector given by

$$\arg\min_{\bar{\mathbf{s}}} \left\{ \left\| \mathbf{y}_{sr}(n) - \sqrt{G_{sr}E_s} \sum_{q=0}^{Q} \mathbf{D}(w_q)\mathbf{H}_{sr,q}^{(0)}(n)\boldsymbol{\Theta}\bar{\mathbf{s}} \right\|^2 \right\} \quad (17)$$

with $\bar{\mathbf{s}}$ as all the possible signal block combinations. We implement "ideal DF" at the relay [21], and the relay then forwards a fresh decoded copy of the received precoded signal, i.e., $\dot{\mathbf{u}}(n)$. The received signal during the relaying phase at the destination is then

$$\mathbf{y}_{rd}(n) = \sqrt{G_{rd}E_s}\,\dot{\boldsymbol{\Phi}}(n)\mathbf{h}_{rd}(n) + \mathbf{n}_{rd}(n) \quad (18)$$

where $\mathbf{n}_{rd}(n)$ is the associated R → D AWGN vector with entries of zero mean and $N_0/2$ variance. $\dot{\boldsymbol{\Phi}}(n) =$
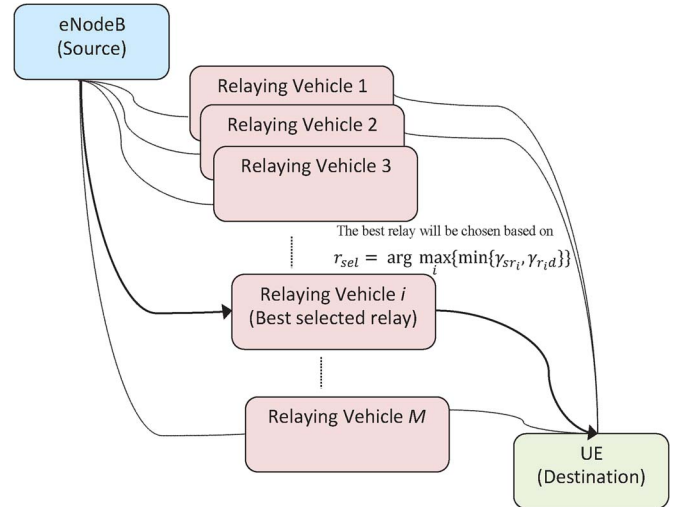

Fig. 3. Best relaying vehicle selection.

$[\mathbf{D}(w_0)\dot{\mathbf{U}}(n) \cdots \mathbf{D}(w_Q)\dot{\mathbf{U}}(n)]$. Finally, arranging (16) and (18) in matrix form, we have

$$\underbrace{\begin{bmatrix} \mathbf{y}_{sd}(n) \\ \mathbf{y}_{rd}(n) \end{bmatrix}}_{\mathbf{Y}(n)} = \sqrt{E_s} \underbrace{\begin{bmatrix} \boldsymbol{\Phi}(n) & 0 \\ 0 & \sqrt{G_{rd}}\dot{\boldsymbol{\Phi}}(n) \end{bmatrix}}_{\mathbf{S}(n)} \underbrace{\begin{bmatrix} \mathbf{h}_{sd}(n) \\ \mathbf{h}_{rd}(n) \end{bmatrix}}_{\mathbf{h}(n)}$$

$$+ \underbrace{\begin{bmatrix} \mathbf{n}_{sd}(n) \\ \mathbf{n}_{rd}(n) \end{bmatrix}}_{\mathbf{n}(n)}. \quad (19)$$

ML detection is then performed at the destination with the following metric:

$$\arg\min_{\bar{\mathbf{s}}} \left\{ \left\| \mathbf{y}_{sd}(n) - \sqrt{E_s} \sum_{q=0}^{Q} \mathbf{D}(w_q)\mathbf{H}_{sd,q}^{(0)}(n)\boldsymbol{\Theta}\bar{\mathbf{s}} \right\|^2 \right.$$

$$\left. + \left\| \mathbf{y}_{rd}(n) - \sqrt{G_{rd}E_s} \sum_{q=0}^{Q} \mathbf{D}(w_q)\mathbf{H}_{rd,q}^{(0)}(n)\dot{\bar{\mathbf{u}}} \right\|^2 \right\} \quad (20)$$

with $\dot{\bar{\mathbf{u}}}$ as all the possible block combinations for the relayed signal. Please note that the orthogonal receive diversity uses the maximal ratio combiner protocol, which is equivalent to the ML detection metric [22], [23].

The aforementioned signal model developed for single relay can be easily extended for a multirelay scenario with relay selection. Let $\dot{\gamma}_{sd}(n)$, $\dot{\gamma}_{sr}(n)$, and $\dot{\gamma}_{rd}(n)$ denote the average end-to-end SNRs per block for the S → D, S → R_i, and R_i → D links, respectively. As shown in Fig. 3, the best relay will be chosen based on

$$r_{\text{sel}} = \arg\max_{r_i} \left\{ \min\left(\dot{\gamma}_{sr_i}, \dot{\gamma}_{r_id} \right) \right\} \quad (21)$$

with r_{sel} as the selected relaying vehicle. We have (21) as a well-known "bound" to the SNR best relay selection method [24], [25]. It was proved, i.e., in [27], that the performance metrics (i.e., diversity gains, bit error rate (BER), PEP, throughput, capacity, etc.) for the cooperative transmission are bounded by the minimum SNR of the S → R and R → D links, and then,

the selection is done by selecting the maximum of the minimal SNR of the cooperating vehicles' S → R and R → D links. The received signal matrix has a similar form as in (19).

III. PAIRWISE ERROR PROBABILITY DERIVATION AND DIVERSITY GAIN ANALYSIS

Here, we investigate the achievable diversity gain of the precoded cooperative communication using the best relaying vehicle. We assume perfect channel state information (CSI) at the relay and the destination. For the orthogonal cooperative protocol with DF relaying, after removing the block index n for mathematical convenience, the PEP at the destination node is given by [21]

$$P_{R_{sel}}\left(\mathbf{S}\to\hat{\mathbf{S}}\Big|\mathbf{h}_{sd},\mathbf{h}_{sr_i},\mathbf{h}_{r_id}\right) \leq P_{\text{Coop}_i}\left(\mathbf{S}\to\hat{\mathbf{S}}\Big|\mathbf{h}_{sd},\mathbf{h}_{r_id}\right)$$
$$+ P_{sr_i}\left(\mathbf{S}\to\hat{\mathbf{S}}\Big|\mathbf{h}_{sr_i}\right)P_{sd}\left(\mathbf{S}\to\hat{\mathbf{S}}\Big|\mathbf{h}_{sd}\right) \quad (22)$$

with $\hat{\mathbf{S}}$ representing the erroneously decoded data matrix instead of the originally transmitted $\mathbf{S}$. $P_{R_{sel}}(\mathbf{S}\to\hat{\mathbf{S}})$ is the end-to-end PEP, $P_{sr_i}(\mathbf{S}\to\hat{\mathbf{S}})$ is the PEP results from the S → R_i link, $P_{sd}(\mathbf{S}\to\hat{\mathbf{S}})$ is the PEP results from the R → D link, and $P_{\text{Coop}_i}(\mathbf{S}\to\hat{\mathbf{S}})$ is the PEP results from the cooperative link (i.e., S → R_i and R_i → D, in the case that the relay detects the signal correctly but the signal resulting from the cooperative link is detected wrong). The conditional PEP for each individual term in (22) is given by [26]

$$P(\mathbf{S}\to\hat{\mathbf{S}}|\mathbf{h}) = Q\left(\sqrt{\frac{1}{2N_0}d^2(\mathbf{S},\hat{\mathbf{S}}|\mathbf{h})}\right). \quad (23)$$

Using the lower bounds recently proposed in [28], (23) can be tightly lower bounded by

$$P(\mathbf{S}\to\hat{\mathbf{S}}|\mathbf{h}) \approx \sum_{m=1}^{3}\varepsilon_m e^{\left(-\frac{\rho_m}{4N_0}d^2(\mathbf{S},\hat{\mathbf{S}}|\mathbf{h})\right)} \quad (24)$$

where $\varepsilon_1 = \varepsilon_2 = 2\varepsilon_3 = 1/12$, $\rho_1 = 12(\sqrt{3}-1)/\pi$, $\rho_2 = 4(3-\sqrt{3})/\pi$, and $\rho_3 = 2\sqrt{3}/\pi$. The Euclidean distance conditioned on the fading channel coefficients is $d^2(\mathbf{S}\to\hat{\mathbf{S}}|\mathbf{h}) = \mathbf{h}^H(\mathbf{S}-\hat{\mathbf{S}})^H(\mathbf{S}-\hat{\mathbf{S}})\mathbf{h}$. Starting with $P_{\text{Coop}_i}(\mathbf{S}\to\hat{\mathbf{S}}|\mathbf{h})$, (24) can be rewritten as

$$P_{\text{Coop}_i}(\mathbf{S}\to\hat{\mathbf{S}}|\mathbf{h}) \approx \sum_{m=1}^{3}\varepsilon_m e^{\left(-\frac{\mathbf{h}_{sd}^H\boldsymbol{\chi}\mathbf{h}_{sd}+G_{r_id}\mathbf{h}_{r_id}^H\boldsymbol{\chi}\mathbf{h}_{r_id}}{4}\rho_m\gamma\right)} \quad (25)$$

where $\boldsymbol{\chi} = (\boldsymbol{\Phi}-\hat{\boldsymbol{\Phi}})^H(\boldsymbol{\Phi}-\hat{\boldsymbol{\Phi}})$. Note that the channel autocorrelation matrix is given by $\mathbf{C}_{h,sd} := \mathbb{E}[\mathbf{h}_{sd}\mathbf{h}_{sd}^H]$, and the channel rank is $r_a := \text{rank}(\mathbf{C}_{h,sd}) \leq (\mathcal{Q}_{sd}+1)(L_{sd}+1)$. For the S → D link, we have $\mathcal{Q}_{sd} = 0$ and $r_a \leq (L_{sd}+1)$. Using the eigenvalues decomposition of the autocorrelation matrix, we have $\mathbf{C}_{h,sd} = \mathbf{V}_{sd}\mathbf{D}_{sd}\mathbf{V}_{sd}^H$, where $\mathbf{D}_{sd} := \text{diag}[\sigma_0^2, \sigma_1^2, \ldots, \sigma_{r_a-1}^2]$ and $\mathbf{V}_{sd}\mathbf{V}_{sd}^H = \mathbf{I}_{r_{sd}}$. Let the normalized channel vector be denoted by $\bar{\mathbf{h}}_{sd}$ of size $r_a \times 1$, whose entries are independent and identically distributed (i.i.d.) Gaussian random variables

with zero mean and unit variance. We can replace $\mathbf{h}_{sd}$ with $\mathbf{V}_{sd}\mathbf{D}_{sd}^{1/2}\bar{\mathbf{h}}_{sd}$ since both will have an identical distribution; thus, the PEP will remain statistically invariant. Further define $\mathbf{A}_{sd} := (\mathbf{V}_{sd}\mathbf{D}_{sd}^{1/2})^H\boldsymbol{\chi}\mathbf{V}_{sd}\mathbf{D}_{sd}^{1/2}$, where $\mathbf{A}_{sd}$ is Hermitian (i.e., $\mathbf{A}_{sd} = \mathbf{A}_{sd}^H$); thus, there exist a unitary matrix $\bar{\mathbf{V}}_{sd}$ and a real nonnegative definite matrix $\bar{\mathbf{D}}_{sd}$ such that $\bar{\mathbf{V}}_{sd}^H\mathbf{A}_{sd}\bar{\mathbf{V}}_{sd} := \bar{\mathbf{D}}_{sd}$. The eigenvector of $\mathbf{A}_{sd}$ is $\bar{\mathbf{D}}_{sd} := \text{diag}[\lambda_0, \lambda_1, \ldots, \lambda_{r_a-1}]$. Since $\bar{\mathbf{V}}_{sd}$ is unitary, the vector $\tilde{\mathbf{h}}_{sd} = \bar{\mathbf{V}}_{sd}\bar{\mathbf{h}}_{sd}$ will have a correlation matrix identical to $\bar{\mathbf{h}}_{sd}$, namely, we have $\tilde{\mathbf{C}} := \mathbb{E}[\tilde{\mathbf{h}}_{sd}\tilde{\mathbf{h}}_{sd}^H] = \mathbb{E}[\bar{\mathbf{V}}_{sd}\bar{\mathbf{h}}_{sd}\bar{\mathbf{h}}_{sd}^H\bar{\mathbf{V}}_{sd}^H]$. From (25), we have

$$P_{\text{Coop}_i}(\mathbf{S}\to\hat{\mathbf{S}}|\mathbf{h})$$
$$\approx \sum_{m=1}^{3}\varepsilon_m e^{-\left(\frac{G_{r_id}\mathbf{h}_{r_id}^H\boldsymbol{\chi}\mathbf{h}_{r_id}}{4}+\frac{\tilde{\mathbf{h}}_{sd}^H\mathbf{A}_{sd}\tilde{\mathbf{h}}_{sd}}{4}\right)\rho_m\gamma}. \quad (26)$$

Following similar steps, we obtain $P_{sd}(\mathbf{S}\to\hat{\mathbf{S}}\|\mathbf{h}_{sd})$ and $P_{sr_i}(\mathbf{S}\to\hat{\mathbf{S}}\|\mathbf{h}_{sr_i})$, and substituting in (22), we have

$$P_{R_{sel}}\left(\mathbf{S}\to\hat{\mathbf{S}}\Big|\mathbf{h}_{sd},\mathbf{h}_{sr_i},\mathbf{h}_{r_id}\right)$$
$$\leq \sum_{m=1}^{3}\varepsilon_m e^{-\frac{\gamma_{sd}}{4}\rho_m\gamma}\left(e^{-\frac{\gamma_{sr_i}}{4}\rho_m\gamma}+e^{-\frac{\gamma_{r_id}}{4}\rho_m\gamma}\right) \quad (27)$$

where $\gamma_{sd} = \mathbf{h}_{sd}^H\boldsymbol{\chi}\mathbf{h}_{sd} = \sum_{p=0}^{r_{sd}-1}\lambda_p|\beta_p^{sd}|^2$, $\gamma_{sr_i} = G_{sr_i}\mathbf{h}_{sr_i}^H \times \boldsymbol{\chi}\mathbf{h}_{sr_i} = G_{sr_i}\sum_{k=0}^{r_{sr_i}-1}\alpha_k|\beta_k^{sr_i}|^2$, and $\gamma_{r_id} = G_{r_id}\mathbf{h}_{r_id}^H \times \boldsymbol{\chi}\mathbf{h}_{r_id} = G_{r_id}\sum_{j=0}^{r_{r_id}-1}\kappa_j|\beta_j^{r_id}|^2$. Define $\gamma_i = \min_i(\gamma_{sr_i}, \gamma_{r_id})$ and $\gamma_i' = \max_i(\gamma_{sr_i}, \gamma_{r_id})$. Note that $-\infty \leq (\gamma_i - \gamma_i') \leq 0$. Based on the analysis of the single relay scenario, by selecting a relay that is close to the destination [27], $G_{sr_i} \ll G_{r_id}$ and $\gamma_i \ll \gamma_i'$. We can rewrite (27) as

$$P_{R_{sel}}\left(\mathbf{S}\to\hat{\mathbf{S}}\Big|\dot{\gamma}_{sd},\dot{\gamma}_b\right) \leq \sum_{m=1}^{3}\varepsilon_m e^{-\rho_m\frac{\dot{\gamma}_{sd}+\dot{\gamma}_b}{4}} \quad (28)$$

where $\dot{\gamma}_{sd} = \gamma\gamma_{sd}$ is the SNR results from the S → D link. $\dot{\gamma}_b = \arg\max_{r_i}(\dot{\gamma}_i)$, i.e., $\dot{\gamma}_i = \gamma^{d_i}\gamma_i$, is the SNR results from the relaying link S → R_i → D, where $d_i = \min(r_{sr}, r_{rd})$. Define $\dot{\gamma} = \dot{\gamma}_{sd} + \dot{\gamma}_b$ as the total end-to-end SNR. The cdf of $\dot{\gamma}_i$ is given by [29]

$$F_{\dot{\gamma}_i}(x) = 1 - P_{sr_i}\left(\mathbf{S}\to\hat{\mathbf{S}}\Big|\gamma_{sr_i} > x\right)$$
$$\times P_{r_id}\left(\mathbf{S}\to\hat{\mathbf{S}}\Big|\gamma_{r_id} > x\right). \quad (29)$$

In (29), $\dot{\gamma}_{sr_i}$ and $\dot{\gamma}_{r_id}$ are a summation of weighted independent exponential distributed random variables and follow the hypoexponential distribution, which is also known as the generalized Erlang distribution, and will have the pdf's given in [30] and [31]. The pdf of $\dot{\gamma}_i$ can then be calculated and results in the form

$$f_{\gamma_i}(x) = \sum_{j_1=0}^{r_{sr_i}-1}\sum_{j_2=0}^{r_{r_id}-1}\left(c_{i,j_1,j_2}\left(\alpha_{i,j_1}+\kappa_{i,j_2}\right)e^{-\left(\alpha_{i,j_1}+\kappa_{i,j_2}\right)x}\right) \quad (30)$$

where

$$c_{i,j_1,j_2} = \left(\prod_{\substack{k \neq j_1 \\ k=0}}^{r_{sr_i}-1} \frac{\alpha_{i,k}}{(\alpha_{i,k} - \alpha_{i,j_1})} \right) \left(\prod_{\substack{k \neq j_2 \\ k=0}}^{r_{r_i d}-1} \frac{\kappa_{i,k}}{(\kappa_{i,k} - \kappa_{i,j_2})} \right).$$

(31)

The average SNR for the relaying link $S \rightarrow R_i \rightarrow D$ is given by $\bar{\gamma}_i = \mathbb{E}[\dot{\gamma}_i]$. Recalling the definition of $\dot{\gamma}_b = \max_i(\dot{\gamma}_i)$, we have

$$F_{\dot{\gamma}_b}(x) = P\left(\max_{i \in R}(\dot{\gamma}_i) < x \right) = \prod_{i=1}^{R} P(\dot{\gamma}_i < x) \qquad (32)$$

where $P(\dot{\gamma}_i < x)$ is given by

$$P(\dot{\gamma}_i < x) = \int_0^x f_{\dot{\gamma}_i}(z)dz$$
$$= \frac{1}{\bar{\gamma}_i} \sum_{j_1=0}^{r_{sr_i}-1} \sum_{j_2=0}^{r_{r_i d}-1} \left(c_{i,j_1,j_2} - c_{i,j_1,j_2} e^{-\left(\alpha_{i,j_1} + \kappa_{i,j_2} \right)x} \right).$$

(33)

Noting $\sum\sum c_{i,j_1},j_2 = 1$ [31], from (32) and (33), we obtain

$$F_{\dot{\gamma}_b}(x) = \prod_{i=1}^{R} \left(\frac{1}{\bar{\gamma}_i} - \frac{1}{\bar{\gamma}_i} \sum_{j_1=0}^{r_{sr_i}-1} \sum_{j_2=0}^{r_{r_i d}-1} \left(c_{i,j_1,j_2} e^{-\left(\alpha_{i,j_1} + \kappa_{i,j_2} \right)x} \right) \right).$$

(34)

In the following, we consider two cases: 1) i.i.d. channels and 2) independent and nonidentically distributed (i.n.i.d.) channels. For the i.i.d. case, we derive the unconditional PEP by averaging (28) and using the binomial theorem [32] along with some mathematical manipulations; note that the relay index i has been removed for the sake of presentation, and the pdf for the end-to-end SNR is $f_{\dot{\gamma}}(x) = f_{\dot{\gamma}_{sd}}(x) * f_{\dot{\gamma}_b}(x)$. The resulting PEP is given by

$$P_i(\mathbf{S} \rightarrow \hat{\mathbf{S}}) \leq \sum_{m=1}^{3} \varepsilon_m A \sum_{p_7=0}^{r_{sd}-1} \sum_{j_3=0}^{M-1} \left(B_{j_3} \sum_{p_5=0}^{r_{sr}-1} \sum_{p_6=0}^{r_{rd}-1} \mathcal{G}_1 \right) \quad (35)$$

with

$$A = \frac{M}{(\bar{\gamma})^M} \sum_{j_1=0}^{r_{sr}-1} \sum_{j_2=0}^{r_{rd}-1} (\alpha_{j_1} + \kappa_{j_2}) \qquad (36)$$

$$B_{j_3} = \binom{M-1}{j_3} (-1)^{j_3} \left(\prod_{p_3=0}^{r_{sr}-1} \prod_{p_4=0}^{r_{rd}-1} c_{p_3,p_4}^{j_3} \right). \qquad (37)$$

We have D_{j_3,p_5,p_6,p_7} and $\mathcal{G}_1$, as defined in following equations:

$$D_{j_3,p_5,p_6,p_7}$$
$$= \frac{1}{\left(1 + \gamma(\alpha_{p_5} + \kappa_{p_6}) - \gamma j_3 \sum_{p_1=0}^{r_{sr}-1} \sum_{p_2=0}^{r_{rd}-1} (\alpha_{p_1} + \kappa_{p_2}) \right)}$$

$$\times \prod_{\substack{k \neq p_7 \\ k=0}}^{r_{r_i d}-1} \frac{\lambda_k}{(\lambda_k - \lambda_{p_7})} \qquad (38)$$

$$\mathcal{G}_1 = D_{j_3,p_5,p_6,p_7}$$
$$\times \left(\frac{4}{1 + 4(\alpha_{p_5} + \kappa_{p_6}) + 4j_3 \sum_{p_1=0}^{r_{sr}-1} \sum_{p_2=0}^{r_{rd}-1} (\alpha_{p_1} + \kappa_{p_2})} \right.$$
$$\left. - \frac{4\rho_m \gamma}{4 + \rho_m \lambda_{p_7} \gamma} \right). \qquad (39)$$

Likewise, for the i.n.i.d. case, we have $P_{\text{ni}}(\mathbf{S} \rightarrow \hat{\mathbf{S}})$, as shown in the following equation:

$$P_{\text{ni}}(\mathbf{S} \rightarrow \hat{\mathbf{S}})$$
$$\leq \sum_{m=1}^{3} \varepsilon_m \sum_{j_3=0}^{r_{sd}-1} \sum_{k=1}^{M} \sum_{p_1=1}^{M-k+1} \sum_{p_2=p_1+1}^{M-k+2} \cdots \sum_{p_k=p_{k-1}+1}^{M} \frac{(-1)^{k+1}}{\lambda_{j_3}\gamma}$$
$$\times \prod_{i=1}^{k} \left(\frac{1}{\bar{\gamma}_i} \sum_{j_1=0}^{r_{sr_{p_i}}-1} \sum_{j_2=0}^{r_{r_{p_i} d}-1} A_{i,j_1,j_2} T_{i,j_1,j_2} \right) \qquad (40)$$

where

$$A_{i,j_1,j_2,j_3} = \left(\frac{4\rho_m \gamma}{4 + \lambda_{j_3} \rho_m \gamma} - \frac{4}{1 + 4(\alpha_{p_i,j_1} + \kappa_{p_i,j_2})} \right)$$

$$T_{p_i,j_1,j_2} = \frac{\rho_m \gamma(\alpha_{p_i,j_1} + \kappa_{p_i,j_2}) c_{i,j_1,j_2}}{\rho_m \gamma(\alpha_{p_i,j_1} + \kappa_{p_i,j_2}) - 1}.$$

From (35) and (40), assuming sufficiently high SNR, we find that the asymptotic diversity gain $D_{\text{gain},M}$ is given by

$$D_{\text{gain},M} = r_{sd} + M(\min(r_{sr}, r_{rd})). \qquad (41)$$

The diversity gain is a function of the number of relaying vehicles involved in the best relay selection, as well as the channel order of all the underlying links.

IV. MAXIMUM DISTANCE FOR MULTIHOP COMMUNICATION

Wireless transmission is constrained by a regulated transmission power, which limits the coverage area. We show that using cooperative transmission can improve the quality of received signal, in addition to extending the coverage area. The outage probability P_{out} is the probability that the error probability exceeds a specified value $\dot{\gamma}_{\text{th}}$. Mathematically speaking, $P_{\text{out}} = \int_0^{\dot{\gamma}_{th}} f_{\dot{\gamma}}(\dot{\gamma})d\dot{\gamma}$ [33], which is the cdf of $\dot{\gamma}$, namely, $F_{\dot{\gamma}}(\dot{\gamma}_{th})$. By defining our unnormalized aggregate channel model that takes into account both path loss and small-scale fading, the relative geometrical gains are redefined as $G_{sd} = d_{sd}^{-\alpha}$, $G_{sr} = d_{sr}^{-\alpha}$, and $G_{rd} = d_{rd}^{-\alpha}$. These can be related to one another through the cosine theorem $G_{sr}^{-2/\alpha} + G_{rd}^{-2/\alpha} - 2G_{sr}^{-1/\alpha}G_{rd}^{-1/\alpha}\cos\theta = G_{sd}^{-2/\alpha}$ and assuming a normalized

gain for a 1-m distance [34]. Hence, $\gamma_{sd} = G_{sd}\mathbf{h}_{sd}^{\mathrm{H}}\boldsymbol{\chi}\mathbf{h}_{sd} = G_{sd}\sum_{p=0}^{\mathrm{R}_{sd}-1}\lambda_p|\beta_p^{sd}|^2$. From (40) and the definition of cdf, the outage probability is given by

$$
\begin{aligned}
&P_{\mathrm{out,co}} \\
&= \sum_{m=1}^{3}\varepsilon_m \sum_{k=1}^{M}\sum_{p_1=1}^{M-k+1}\sum_{p_2=p_1+1}^{M-k+2}\cdots\sum_{p_k=p_{k-1}+1}^{M}\frac{(-1)^{k+1}}{\rho_m\gamma}\prod_{i=1}^{k}\Psi_i
\end{aligned}
\tag{42}
$$

where

$$
\begin{aligned}
\Psi_i = \sum_{j_1=0}^{\mathrm{R}_{sr_{p_i}}-1}\sum_{j_2=0}^{\mathrm{R}_{r_{p_i}d}-1}T_{i,j_1,j_2}\bigg(&\rho_m\gamma\left(1-e^{\left(-\frac{1}{\rho_m\gamma}\right)\dot{\gamma}_{th}}\right) \\
&-\frac{1}{(\alpha_{p_i,j_1}+\kappa_{p_i,j_2})}\left(1-e^{-(\alpha_{p_i,j_1}+\kappa_{p_i,j_2})\dot{\gamma}_{th}}\right)\bigg).
\end{aligned}
\tag{43}
$$

From (42), d_{sd} can be shown as an effective parameter on the resulting outage probability of our proposed scheme.

V. SIMULATION RESULTS AND DISCUSSION

Here, we present numerical results to demonstrate the error rate and outage probability performance. LTE-A targets peak data rates up to 1 Gb/s with up to 100 MHz supported spectrum bandwidth and by making use of high-order multiple antenna transmission. Unless otherwise stated, we consider quaternary phase-shift keying modulation and assume $f_c = 2.5$ GHz, $T_s = 500$ μs, $v_r = 60$ km/h, $\alpha = 3.67$, $\theta = \pi$, $G_{sr}/G_{rd} = -30$ dB, and $\tau_d = 1.328$ μs [5], [35]. We assume that perfect channel state information is available at the receiving terminals. We use the precoder $\boldsymbol{\Theta}$ with parameters $P = 2$ and $Z = 2$. This results in $[L_{\mathrm{Coop}}, \mathcal{Q}_{\mathrm{Coop}}] = [1, 1]$ for S $\to$ R and R $\to$ D links, where $Q_{\mathrm{Coop}} = \min(\mathcal{Q}_{sr}, \mathcal{Q}_{rd})$. A frequency–time flat channel is used for the S $\to$ D link, i.e., $[L_{sd}, \mathcal{Q}_{sd}] = [0, 0]$. Our system and the mathematical model both indicate that the relay is selected somewhere in between the "BS" and the "end-user." Based on the system parameters stated earlier, our resultant transmission was ≈ 48 s in duration before the relaying vehicle approaches the designated end-user's exact location. With approximately 100–150 Mb/s downlink data rate supported by LTE-A high-mobility technology [5], our scheme is capable of transferring large data messages. Larger messages/streaming sizes can be divided into data chunks and distributed over several cooperative relaying links.

In Fig. 4, we illustrate the PEP expression (40) derived for the relay selection case under i.n.i.d channels, as compared with the exact expression (22). Our derived PEP curves are plotted as solid lines, whereas the numerical "exact" PEP curves are plotted as dashed lines. The exact PEP can be found by taking the expectation of the unconditional PEP numerically through the random generation of $\mathbf{h}$ with proper statistics. We assume $M = 1, 2$, and 3 available relaying vehicles with $[L_{\mathrm{Coop}}, \mathcal{Q}_{\mathrm{Coop}}] = [1, 1]$. We observe that the derived PEP provides a tight upper bound on the exact one with about $\simeq 0.5$ dB difference. For high SNR, the overall system performance improves as the achievable diversity increases. So far, we derived designs capable of achieving full diversity. Power savings is clearly
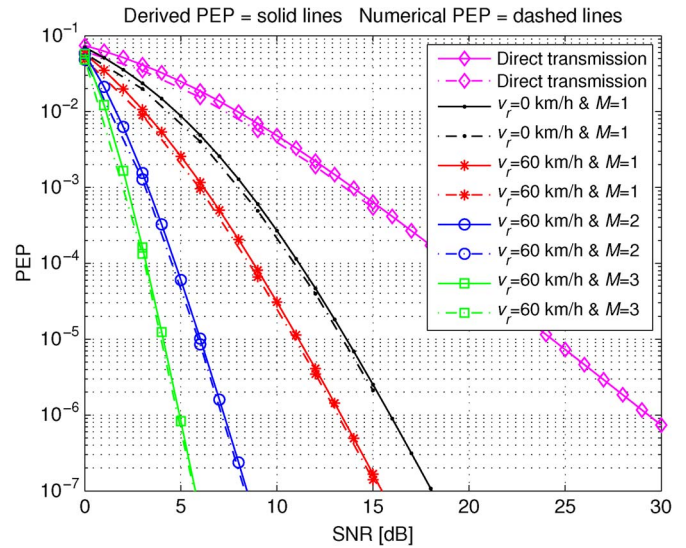

Fig. 4. Comparison of the derived PEP in (40) and exact PEP expressions for cooperative vehicular transmission over the LTE-A case with relay selection.

observed; for example, at PEP $= 10^{-5}$, a transmitting power consumption savings of 5 and 7 dB is observed for $M = 2$ and $M = 3$, respectively, with respect to $M = 1$. To show the effect of the mobility on the error performance rates compared with stationary relays and the direct noncooperative transmissions, we also plot results for these two traditional scenarios. The curves showing direct transmission indicate the traditional transmission without the deployment of the cooperative vehicular relaying, whereas the curves for $v_r = 0$ km/h and single relay $M = 1$ indicate the traditional cooperative transmission for a single stationary relay. Comparing the two traditional scenarios with our best relaying vehicle selection case and using a precoded cooperative transmission to extract the underlying Doppler diversity resulting from the relaying vehicle mobility ($v_r = 0$ km/h and $M = 1, 2$, or 3), a power consumption savings is clearly observed. For example, at PEP $= 10^{-5}$, a transmitting power consumption saving of 10 and 20 dB is observed for $M = 3$ compared with the traditional cooperative relaying and direct transmission scenarios, respectively. Note that the precoder extracts the underlying multipath–Doppler diversities (L and Q); for the plotted curves, we have $L = 1$. However, for the stationary cases ($v_r = 0$ km/h), we have $Q = 0$, whereas for the mobility scenarios ($v_r = 60$ km/h), we have $Q = 1$.

In Fig. 5, we further plot $-\log P(\mathbf{S} \to \hat{\mathbf{S}})/\log(\gamma)$ to precisely observe the slope of the PEPs for the best relay selection scenario, and the achieved asymptotic diversity orders equal to 5, 9, and 13 are achieved. We observe that the results conform to those obtained from the derived expression (41), and the full underlying multipath–Doppler–spatial diversity is extracted. In Fig. 6, we investigate the effect of imperfect channel state information (I-CSI) on the BER of cooperative vehicular relaying schemes through Monte Carlo simulation. A single known pilot symbol is periodically inserted in each input block $\mathbf{s}(n)$. In the I-CSI, we need to estimate the direct S $\to$ D channel and the indirect S $\to$ R $\to$ D channel. We consider the strategy in [36], which is called *cascaded channel estimation*,
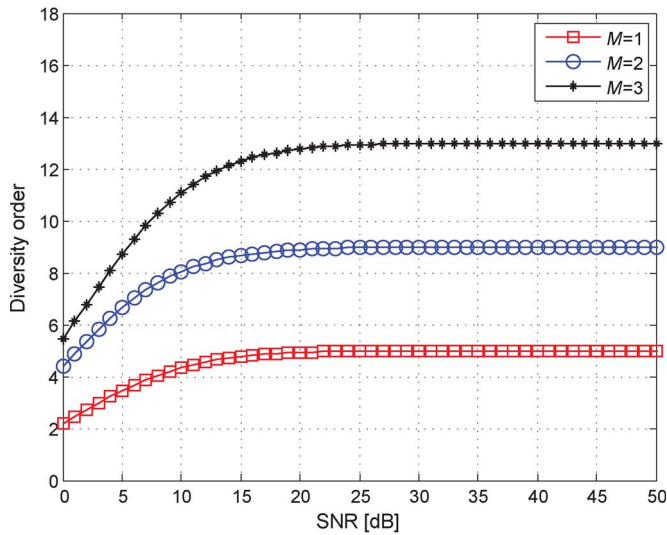
Fig. 5.   Diversity order gains for cooperative vehicular transmission over the LTE-A case with relay selection.
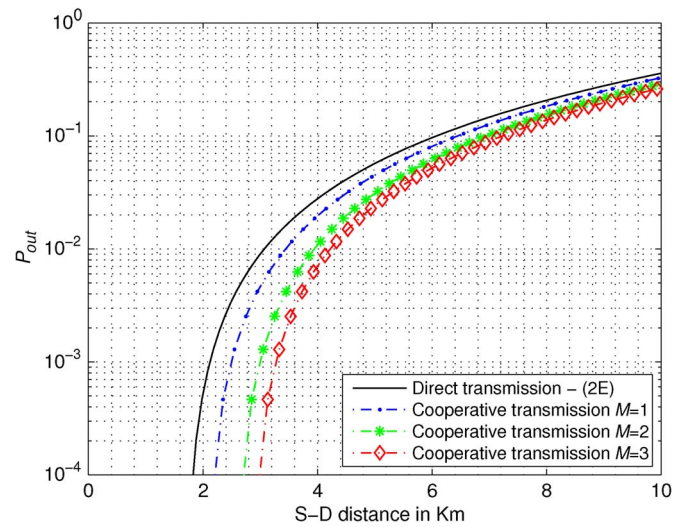

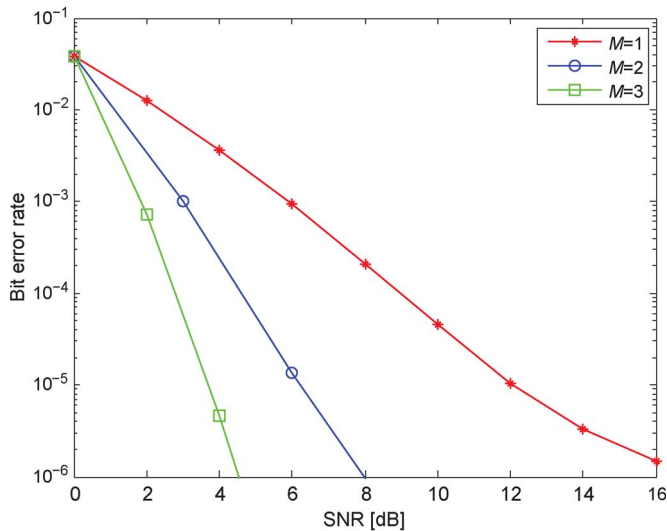Fig. 7.   S → D distance in kilometers versus outage probability.

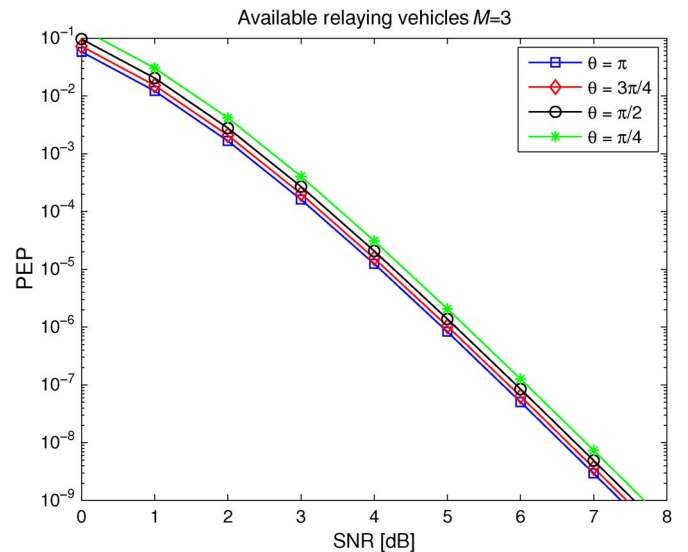Fig. 6.   Effect of imperfect channel estimation on the error rate performance.

Fig. 8.   Effect of changing the S → R and R → D cooperative angle θ.

where the cascaded S → R → D channel is estimated at the destination terminal, avoiding the need for channel estimation at the relay terminal. We adopt the pilot symbol assisted modulation technique [37], which relies on the insertion of known pilot symbols in information-bearing data. The known symbols are periodically inserted into the data sequence. Following the well-known minimum mean square estimation (MMSE) technique, a Wiener filter is used to minimize the variance of the estimation error. The corresponding set of the filter coefficients is optimized for minimizing the estimation error variance. The optimum interpolation coefficient matrix of the estimator and the received pilot vector autocorrelation will then be a function of the channel autocorrelation matrix. A sliding window covering a total of 11 pilots from preceding and following blocks is used for channel estimation of the fading coefficient. It is observed that the imperfect channel estimate degrades the performance for the BER performance, resulting in error floors when no relay selection is performed. This observation of the error floor effect is analytically presented in the Appendix.

The main reason is that the asymptotical performance metrics become independent of γ and result in the presence of an error floor. On the other hand, due to extra spatial diversity achieved by our proposed relay selection scheme, we are able to suppress the error floor in the simulated SNR ranges.

Fig. 7 shows the coverage extension gains for the opportunistic cooperative transmission compared with the direct transmission using the outage probabilities in (42), for $\gamma = 10$ dB and $\dot{\gamma}_{\mathrm{th}} = 5$ dB [38]. For the outage probability of 10^{-4}, coverage extension advantages of $\simeq 1.1, \simeq 1.6$, and $\simeq 1.7$ km are observed for cooperative transmission with $M = 1$, $M = 2$, and $M = 3$, respectively, compared with traditional direct transmission.

The effect of changing the S → R and R → D cooperative angle θ is plotted in Fig. 8. We assume a number of available relays to cooperate in the transmission $M = 3$ and $\theta = (\pi, 3\pi/4, \pi/2, \pi/4)$. The results indicate similar diversity gains with small shifts in the pairwise error curves, indicating tightly closed coding gains (the change in the required SNR to achieve a similar error rate). The optimum transmission angle is at

TABLE I
NUMBER OF DOPPLER SHIFTS Q FOR A GIVEN
BLOCK LENGTH AND $P-Z$ PARAMETERS

$[P, Z]$	Q	Transmitted block length N_t	ML search possibilities. *m is the bits/symbol
$[1, 1]$	1	4	$(m)^4$
$[13, 13]$	2	210	$(m)^{210}$
$[18, 18]$	3	399	$(m)^{399}$
$[22, 22]$	4	598	$(m)^{598}$
$[25, 25]$	5	780	$(m)^{780}$
$[28, 28]$	6	986	$(m)^{986}$
$[31, 31]$	7	1216	$(m)^{1216}$

$\theta = \pi$, indicating that the eNB/BS, the relaying vehicle, and the designated end-user equipment are in a straight alignment.

The result confirms our analytical derivations and closed-form expression and shows that based on the basis expansion model for the time-variant channels (12), the maximum diversity order of time-selective channels depends on the number of bases. The linearly precoded transmissions maximize the available Doppler diversity order and efficiently implementable transmissions that are designed to enable the maximum achievable multipath–Doppler diversity order, which turned out to be the rank of the underlying channel correlation matrix. In our study, we assume precoder parameters of $P = 2$ and $Z = 2$. Hence, the input data block $\mathbf{s}(n)$ is of length $N_s \times 1$ (i.e., PZ), and the output of the precoder $\mathbf{u}(n)$ is of length $N_t \times 1$ (i.e., $(P + Q)(Z + L)$). We then have the precoder output rate equal to $N_s/N_t = PZ/((P + Q)(Z + L))$. It is clear that increasing the precoder output rate can be achieved by increasing P and/or Z. This comes at the expense of higher system complexity (mainly received signal detection), as the length of transmitted/received blocks is increased. Furthermore, the diversity order is a function of the channel order $(Q + 1)(L + 1)$. From the definition of P and Z, we have $Q(1 - (Z + L)T_s f_d) - 1 < P(Z + L)T_s f_d \leq Q(1 - (Z + L)T_s f_d)$. Hence, we can choose P and Z to satisfy a minimum required Q, as shown in Table I. The diversity order is then a function of the fading channel delay spread, the Doppler shifts (the relative mobility), the symbol duration, and the precoder design (i.e., dimensions). In many communication problems, ML detection reduces to solving an integer least squares problem, i.e., a search for the closest integer lattice point to the given vector, and the N_t-dimensional vectors will have to span the N_t-dimensional lattice. Applications involving higher speed vehicles and/or those with large precoder dimensions result in a large search space for ML, rendering ML computationally intractable. In such cases, sphere detection techniques [39] can be used.

VI. CONCLUSION

We propose an enabling cooperative vehicular relaying transmission scheme to contribute toward the formation of an advanced heterogeneous telecommunication network to provide increased networking capabilities for heavily populated urban areas. Our transmission scheme makes use of vehicles equipped with low elevation antennas and short- and medium-range wireless communication technologies, allowing new functionalities and capabilities. To realize the full potential of the proposed

architecture, we conduct an in-depth investigation of performance limits and gains, as well as development of enabling techniques to support such broadband transmission. We demonstrate that using vehicles for cooperative relaying in broadband cellular networks not only potentiates reduced levels of power consumption but also provides higher throughput, increases coverage, lowers operational and capital expenditures, allows for faster roll out, and promises more flexibility. Our proposed scheme can be particularly useful in heavily populated urban areas, where we can take advantage of the potentially large number of relaying vehicles to extract extra spatial diversity and assist in the broadband signal transmission.

Our work involves investigating the performance of the proposed cooperative vehicular relaying system over the LTE-A downlink session, in which the eNodeB point communicates with a UE using cooperating vehicles as relaying terminals, where best relay selection is deployed. For the doubly selective (time- and frequency-selective) vehicular channel under consideration, we employ a precoded cooperative transmission technique to extract the underlying rich multipath–Doppler–spatial diversity. We derive a closed-form expression for the PEP as a benchmark to assess our analysis and future research studies of such an approach, as well the derivation of the outage probability expression. We further conduct Monte Carlo simulations against analytical derivations and present the error rate performance under various mobility scenarios. Analytical and simulation results demonstrate significant performance gains, where notable diversity gains are achieved, as well as a notable reduction in error rates. Additionally, a reduction in the required transmitting powers compared with traditional transmission schemes is observed. The coverage distance gains are analyzed using our outage probability expression, indicating the advantage of our proposed transmission technique over traditional transmissions. The effect of I-CSI is also studied through an asymptotical PEP analysis. We mathematically proved the existence of an error floor on the performance metrics under the I-CSI assumption for such scenarios. Our results show that I-CSI severely degrades the performance for low diversity gain transmission when assuming a single relaying vehicular deployment and results in error floors. However, due to extra spatial diversity extracted when using our transmission technique with multiple relaying vehicles, our scheme shows superior performance in suppressing the error floor for various SNR ranges.

APPENDIX
PAIRWISE ERROR PROBABILITY WITH IMPERFECT CHANNEL ESTIMATION

Here, we analyze the effect of imperfect channel state information of the PEP expression. We consider the PEP of the cooperative S → D and S → R → D(25). Let $\mathbf{e}_{sd}$ and $\mathbf{e}_{srd} = \mathbf{e}_{sr}\mathbf{e}_{rd}$ denote the imperfect channel information/estimation error vectors for the associated links. Therefore, we can write

$$\underbrace{[\hat{\mathbf{h}}_{sd} \quad \hat{\mathbf{h}}_{srd}]^{\mathrm{H}}}_{\hat{\mathbf{h}}} = \underbrace{[\mathbf{h}_{sd} \quad \mathbf{h}_{srd}]^{\mathrm{H}}}_{\mathbf{h}} - \underbrace{[\mathbf{e}_{sd} \quad \mathbf{e}_{srd}]^{\mathrm{H}}}_{\mathbf{e}} \quad (A.1)$$

where $\hat{\mathbf{h}}_{sd}$ and $\hat{\mathbf{h}}_{srd} = \hat{\mathbf{h}}_{sr}\hat{\mathbf{h}}_{rd}$ are the "estimated" channel vectors for the direct S → D channel and the indirect S →

R → D channel, respectively. In the case of imperfect channel estimation, the output of the ML detector at the destination terminal can be expressed as

$$\mathbf{Y}_C = \hat{\mathbf{h}}_Q^{\mathrm{H}} \mathbf{Y} = \sqrt{E_s} \hat{\mathbf{h}}_Q^{\mathrm{H}} \mathbf{h}_Q \mathbf{S} + \hat{\mathbf{h}}_Q^{\mathrm{H}} \mathbf{n} \qquad (\mathrm{A.2})$$

where $\mathbf{h}_Q = \sum_{q=0}^{Q} \mathrm{diag}[\mathbf{D}(w_q), \mathbf{D}(w_q)] \mathrm{diag}[\mathbf{H}_{sd,q}^{(0)}, \mathbf{H}_{srd,q}^{(0)}]$, and $\hat{\mathbf{h}}_Q$ is its estimate related to each other through $\mathbf{h}_Q = \hat{\mathbf{h}}_Q + \mathbf{e}_Q$. The estimate can be further rewritten as

$$\hat{\mathbf{h}}_Q^{\mathrm{H}} = \mathrm{diag}\underbrace{\left[\left(\sum_{q=0}^{Q} \hat{\mathbf{H}}_{sd,q}^{(0)} \right)^{\mathrm{H}}, \left(\sum_{q_3=0}^{Q} \hat{\mathbf{H}}_{srd,q_3}^{(0)} \right)^{\mathrm{H}} \right]}_{\text{Channel matrix}}$$

$$\times \mathrm{diag}\underbrace{\left[(\mathbf{D}(w_q))^{\mathrm{H}}, (\mathbf{D}(w_{q_3}))^{\mathrm{H}} \right]}_{\text{Doppler spread matrix}} \qquad (\mathrm{A.3})$$

where $[\mathbf{H}_{sd,q}^{(0)}(n)]_{k,m} = h_{rd,q}(n; k-m)$ and $[\mathbf{H}_{srd,q}^{(0)}(n)]_{k,m} = h_{sr}(n) h_{rd,q}(n, k-m)$, $k, m \in [0, N_t - 1]$. Since the Doppler spread matrix is calculated with respect to a known velocity, estimation is needed only over the channel matrix. Noting $\mathbf{e}_Q = \sum_{q=0}^{Q} \mathrm{diag}[\mathbf{D}(w_q), \mathbf{D}(w_q)] \times \mathrm{diag}[\mathbf{e}_{h_{sd},q}, \mathbf{e}_{h_{srd},q}]$, where $\mathbf{e}_{h_{sd},q}$ and $\mathbf{e}_{h_{srd},q}$ are the estimation errors for channel matrices $\hat{\mathbf{H}}_{sd,q}^{(0)}$ and $\hat{\mathbf{H}}_{srd,q}^{(0)}$, respectively, we have

$$\mathbf{Y}_C = \sqrt{E_s} \hat{\mathbf{h}}_Q^{\mathrm{H}} \hat{\mathbf{h}}_Q \mathbf{S} + \hat{\mathbf{h}}_Q^{\mathrm{H}} (\sqrt{E_s} \mathbf{e}_Q \mathbf{S} + \mathbf{n}). \qquad (\mathrm{A.4})$$

The second term includes the effect of both noise and imperfect estimation and is zero-mean complex Gaussian with the variance of $E_s \sigma_{\mathbf{e}_Q}^2 + N_0$. The average of the effective SNR $(\hat{\gamma})$, including the effect of both noise and imperfect estimation, is then given by

$$\mathbb{E}(\hat{\gamma}) = \frac{\gamma \left| \sigma_{\mathbf{h}_Q}^2 + \sigma_{\mathbf{e}_Q}^2 - \mathbb{E}(\mathbf{h}_Q \mathbf{e}_Q) \right|}{\gamma \sigma_{\mathbf{e}_Q}^2 + 1} \qquad (\mathrm{A.5})$$

where the estimation error variance vector $\sigma_{\mathbf{e}_Q}^2$ is [37]

$$\sigma_{\mathbf{e}_Q}^2 = \gamma \sigma_{\mathbf{h}_Q}^2 - \mathbf{w}_c^{\mathrm{H}} \mathbf{R}_c^{-1} \mathbf{w}_c \qquad (\mathrm{A.6})$$

we have $\mathbf{w}_c$ and $\mathbf{R}_c$ as the MMSE optimum filter coefficients and the channel autocorrelation, respectively [37]. Using the results from [40], we can rewrite (A.6) as

$$\sigma_{\mathbf{e}_Q}^2 = \left(\left(\frac{\gamma c}{|E|^2} \mathbf{1} \right)^{-1} + |E_s|^2 \tilde{\mathbf{R}}^{\mathrm{H}} \mathbf{I}^{-1} \tilde{\mathbf{R}} \right)^{-1} \qquad (\mathrm{A.7})$$

where $\tilde{\mathbf{R}}$ is the normalized channel autocorrelation.

Under the assumption of the I-CSI, the conditional PEP can be therefore revised as

$$P_{\mathrm{Coop}_i}(\mathbf{S} \to \hat{\mathbf{S}} | \mathbf{h}) \Big|_{\mathrm{I-CSI}} \approx \sum_{m=1}^{3} \varepsilon_m$$

$$\times \exp\left(-\left(\mathbf{h}_{sd}^{\mathrm{H}} \chi \mathbf{h}_{sd} + G_{r_i d} \mathbf{h}_{r_i d}^{\mathrm{H}} \chi \mathbf{h}_{r_i d} \right) \frac{\rho_m \gamma}{4\left(\rho_m \gamma \sigma_{\mathbf{e}_Q}^2 + 1 \right)} \right). \qquad (\mathrm{A.8})$$

For sufficiently high SNR, i.e., by taking the limit of $\gamma \to \infty$, we have

$$\lim_{\gamma \to \infty} P_{\mathrm{Coop}_i}(\mathbf{S} \to \hat{\mathbf{S}} | \mathbf{h}) \Big|_{\mathrm{I-CSI}}$$

$$\approx \sum_{m=1}^{3} \varepsilon_m \exp\left(-\mathbf{h}_{sd}^{\mathrm{H}} \chi \mathbf{h}_{sd} + G_{r_i d} \mathbf{h}_{r_i d}^{\mathrm{H}} \chi \mathbf{h}_{r_i d} \right) \qquad (\mathrm{A.9})$$

which becomes independent of γ and indicates the presence of an error floor. As observed in Fig. 6 and the analytical justification presented in the Appendix, the imperfect channel estimate degrades the performance for the error rate performance, resulting in error floors in the performance curves when no relay selection is performed. The error floor results in wasting the transmitted power, whereas the performance will be saturated at a constant level; in other words, it means that even by increasing the transmitted power, the performance will not be improved. The main reason is that the asymptotical performance metrics become independent of the SNR γ and result in the presence of the error floor. On the other hand, due to extra spatial diversity achieved by our proposed relay selection scheme, we are able to suppress the error floor in the simulated SNR ranges by increasing the number of the involved relays and, hence, extracting additional virtual MIMO spatial diversity.

REFERENCES

[1] M. Naphade, G. Banavar, C. Harrison, J. Paraszczak, and R. Morris, "Smarter cities and their innovation challenges," *IEEE Comput.*, vol. 44, no. 6, pp. 32–39, Jun. 2011.

[2] S. Lee, J. Park, M. Gerla, and S. Lu, "Secure incentives for commercial ad dissemination in vehicular networks," *IEEE Trans. Veh. Technol*, vol. 61, no. 6, pp. 2715–2728, Jul. 2012.

[3] I. K. Fu et al., "Multicarrier technology for 4G WiMax system [WiMAX/LTE Update]," *IEEE Commun. Mag.*, vol. 48, no. 8, pp. 50–58, Aug. 2010.

[4] W. Ni, I. B. Collings, and R. P. Liu, "Relay handover and link adaptation design for fixed relays in IMT-Advanced using a new Markov chain model," *IEEE Trans. Veh. Technol.*, vol. 61, no. 4, pp. 1839–1853, May 2012.

[5] C. Zhang, S. Ariyavisitakul, and M. Tao, "LTE-advanced and 4G wireless communications [Guest Editorial]," *IEEE Commun. Mag.*, vol. 50, no. 2, pp. 102–103, Feb. 2012.

[6] J. Lin, A. Vinel, S. Vassilaras, T. Zhang, and K. Lo, "Special section on telematics advances for vehicular communication networks," *IEEE Trans. Veh. Technol.*, vol. 61, no. 1, pp. 1–2, Jan. 2012.

[7] Q. Wang, P. Fan, and K. B. Letaief, "On the joint V2I and V2V scheduling for cooperative VANETs with network coding," *IEEE Trans. Veh. Technol.*, vol. 61, no. 1, pp. 62–73, Jan. 2012.

[8] F. Dressler, F. Kargl, J. Ott, O. K. Tonguz, and L. Wischof, "Research challenges in intervehicular communication: Lessons of the 2010 Dagstuhl seminar," *IEEE Commun. Mag.*, vol. 49, no. 5, pp. 158–164, May 2011.

[9] H. Ilhan, M. Uysal, and Ã. Altunbas, "Cooperative diversity for intervehicular communication: Performance analysis and optimization," *IEEE Trans. Veh. Technol.*, vol. 58, no. 7, pp. 3301–3310, Sep. 2009.

[10] M. Jerbi, S. M. Senouci, Y. Ghamri-Doudane, and M. Cherif, "Vehicular communications networks: Current trends and challenges," in *Handbook of Research on Next Generation Mobile Networks and Ubiquitous Computing*. Hershey, PA, USA: IGI Global, 2012, pp. 251–262.

[11] M. F. Feteiha and M. Uysal, "Cooperative transmission for broadband vehicular networks over doubly-selective fading channels," *J. IET Commun.*, vol. 6, no. 16, pp. 2760–2768, Nov. 2012.

[12] M. F. Feteiha and M. Uysal., "Multipath–Doppler diversity for broadband cooperative vehicular communications," in *Proc. IEEE Int. Conf. Commun.*, Kyoto, Japan, Jun. 2011, pp. 1–6.

[13] G. Zhang, K. Yang, P. Liu, and X. Feng, "Incentive mechanism for multiuser cooperative relaying in wireless ad hoc networks: A

resource-exchange based approach," *Wireless Pers. Commun.*, vol. 73, no. 3, pp. 697–715, Dec. 2013.

[14] J. Laneman, D. Tse, and G. Wornell, "Cooperative diversity in wireless networks: Efficient protocols and outage behavior," *IEEE Trans. Inf. Theory*, vol. 50, no. 12, pp. 3062–3080, Dec. 2004.

[15] W. C. Jakes, *Microwave Mobile Communications*. New York, NY, USA: Wiley, 1994.

[16] C. S. Patel, G. L. Stuber, and T. G. Pratt, "Simulation of Rayleigh-faded mobile-to-mobile communication channels," *IEEE Commun.*, vol. 53, no. 11, pp. 1876–1884, Nov. 2005.

[17] J. G. Proakis and M. Salehi, *Digital Communications*, 5th ed. New York, NY, USA: McGraw-Hill, 2008.

[18] A. S. Akki and F. Haber, "A statistical model of mobile-to-mobile land communication channel," *IEEE Trans. Veh. Technol.*, vol. VT-35, no. 1, pp. 2–7, Feb. 1986.

[19] J. Soler-Garrido, M. Sandell, and W. H. Chin, "Interference mitigation in an LTE femtocell base station using uplink antenna selection," *EURASIP J. Wireless Commun. Netw.*, vol. 2012, p. 335, Nov. 2012.

[20] X. Ma and G. Giannakis, "Maximum-diversity transmissions over doubly selective wireless channels," *IEEE Trans. Inf. Theory*, vol. 49, no. 7, pp. 1832–1840, Jul. 2003.

[21] Y. Ma, N. Yi, and R. Tafazolli, "Bit and power loading for OFDM-based three-node relaying communications," *IEEE Trans. Signal Process.*, vol. 56, no. 7, pp. 3236–3247, Jul. 2008.

[22] T. Wang and G. B. Giannakis, "Complex field network coding for multiuser cooperative communications," *IEEE J. Sel. Areas Commun.*, vol. 26, no. 3, pp. 561–571, Apr. 2008.

[23] Z. Yi and I. Kim, "Diversity order analysis of the decode-and-forward cooperative networks with relay selection," *IEEE Trans. Wireless Commun.*, vol. 7, no. 5, pp. 1792–1799, May 2008.

[24] S. S. Ikki and M. H. Ahmed, "Performance of multiple-relay cooperative diversity systems with best relay selection over Rayleigh fading channels," *EURASIP J. Adv. Signal Process.*, vol. 2008, pp. 580368-1–580368-7, Mar. 2008.

[25] Y. Jing and H. Jafarkhani, "Single and multiple relay selection schemes and their achievable diversity orders," *IEEE Trans. Wireless Commun.*, vol. 8, no. 3, pp. 1414–1423, Mar. 2009.

[26] V. Tarokh, N. Seshadri, and A. Calderbank, "Space–time codes for high data rate wireless communication: Performance criterion and code construction," *IEEE Trans. Inf. Theory*, vol. 44, no. 2, pp. 744–765, Mar. 1998.

[27] H. Muhaidat and M. Uysal, "Cooperative diversity with multiple-antenna nodes in fading relay channels," *IEEE Trans. Wireless Commun.*, vol. 7, no. 8, pp. 3036–3046, Aug. 2008.

[28] M. Wu, X. Linm, and P. Y. Kam, "New exponential lower bounds on the Gaussian Q-function via Jensen's inequality," in *Proc. IEEE 73rd Veh. Technol. Conf.*, Budapest, Hungary, May 2011, pp. 1–5.

[29] H. Shao and N. C. Beaulieu, "Block coding for impulsive Laplacian noise," in *Proc. IEEE Int. Conf. Commun.*, Cape Town, South Africa, May 2010, pp. 1–6.

[30] M. Ulrey, B. Co, and W. Bellevue, "Formulas for the distribution of sums of independent exponential random variables," *IEEE Trans. Rel.*, vol. 52, no. 2, pp. 154–161, Jun. 2003.

[31] S. M. Ross, *Introduction to Probability and Statistics for Engineers and Scientists,* 3rd ed. San Diego, CA, USA: Academic, 2004.

[32] C. Liu, "The essence of the generalized Newton binomial theorem," *Commun. Nonlinear Sci. Numer. Simul.*, vol. 15, no. 10, pp. 2766–2768, Oct. 2010.

[33] M. K. Simon and M. S. Alouini, *Digital Communication Over Fading Channels,* 2nd ed. Piscataway, NJ, USA: IEEE Press, 2005.

[34] S. Cui, A. J. Goldsmith, and A. Bahai, "Energy-constrained modulation optimization," *IEEE Trans. Wireless Comm.*, vol. 4, no. 5, pp. 2349–2360, Sep. 2005.

[35] I. Sen and D. Matolak, "V2V channels and performance of multiuser spread spectrum modulation," in *Proc. IEEE 66th Veh. Technol. Conf.*, Baltimore, MD, USA, Sep. 2007, pp. 2139–2143.

[36] O. Amin, B. Gedi, and M. Uysal, "Channel estimation for amplify-and-forward relaying: Cascaded versus disintegrated estimators," *IET Commun.*, vol. 4, no. 10, pp. 1207–1216, Jul. 2010.

[37] J. K. Cavers, "An analysis of pilot symbol assisted modulation for Rayleigh fading channels [mobile radio]," *IEEE Trans. Veh. Technol.*, vol. 40, no. 4, pp. 686–693, Nov. 1991.

[38] D. S. Michalopoulos, A. S. Lioumpas, G. K. Karagiannidis, and R. Schober, "Selective cooperative relaying over time-varying channels," *IEEE Trans. Commun.*, vol. 58, no. 8, pp. 2402–2412, Aug. 2010.

[39] O. Damen, A. Chkeif, and J. Beltore, "Lattice code decoder for space–time codes," *IEEE Commun. Lett.*, vol. 4, no. 5, pp. 161–163, May 2000.

[40] S. M. Kay, *Fundamentals of Statistical Signal Processing: Estimation Theory*. Englewood Cliffs, NJ, USA: Prentice-Hall, 1993.

Mohamed F. Feteiha (S'10–M'12) received the B.Eng. and M.Eng. degrees (both with Excellence grade with Honor) in telecommunications engineering from the Arab Academy for Science and Technology and Maritime Transport, Alexandria, Egypt, in 1999 and 2006, respectively, and the Ph.D. degree in electrical and computer engineering from the University of Waterloo, Waterloo, ON, Canada, in 2012.

He is an Assistant Professor and a Researcher with the Informatics Research Institute (IRI), City of Scientific Research and Technological Applications (CSRTA), Alexandria. He is a Visiting Researcher and was previously a Postdoctoral Research Fellow and Team Leader with the Telecommunications Research Lab, Queen's University, Kingston, ON. He is working in the area of wireless networks architecture, deployments, and performance evaluation. In 2012, he was a Research and Teaching Associate with the Wireless Communication Systems (WiComS) Research Lab, University of Waterloo. From 2000 to 2008, he was an Assistant Researcher with IRI-CSRTA. During this period, he intensively worked on distributed and wireless systems and networks. His record spans more than 20 publications as a first author in top IEEE journals and conferences.

Hossam S. Hassanein (S'86–M'90–SM'06) received the Ph.D. degree in computing science from the University of Alberta, Edmonton, AB, Canada, in 1990.

He is a leading authority in the areas of broadband, wireless and mobile networks architecture, protocols, control, and performance evaluation. His record spans more than 500 publications in journals, conferences, and book chapters, in addition to numerous keynotes and plenary talks at flagship venues. He is also the Founder and Director of the Telecommunications Research Lab, School of Computing, Queen's University, Kingston, ON, Canada, with extensive international academic and industrial collaborations.

Dr. Hassanein is an IEEE Communications Society Distinguished Speaker (Distinguished Lecturer 2008–2010). He is currently the Chair of the IEEE Communication Society Technical Committee on Ad hoc and Sensor Networks. He has received several recognitions and best papers awards at top international conferences.